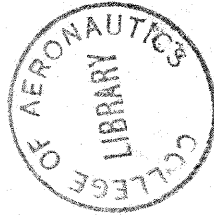


CoA/M/E+C-46

ST. NO. R 28921
U.D.C.
AUTH.

Fourth International Conference of
L'Association Internationale Pour le Calcul
Analogique

Brighton, England, 14th - 18th September, 1964



RESISTANCE NETWORK SIMULATION
OF SEMICONDUCTOR SYSTEMS

- by -

H.W. LOEB

THE COLLEGE OF AERONAUTICS,
DEPARTMENT OF ELECTRICAL AND
CONTROL ENGINEERING,
CRANFIELD, BEDFORDSHIRE.

CoA Memo E and C No. 46
September, 1964.

R 28921

1. Introduction

A basic problem in the design theory of semiconductor systems such as p-n junction devices relates to the determination of the spatial variation of electrostatic potential, ψ , of electric field intensity, and of mobile carrier (hole, electron) concentrations, p and n . These quantities are governed by the system geometry as specified by the 'built-in' concentration profiles of donor and acceptor impurities according to the Shockley-Poisson equation:

$$\nabla^2 \psi = - \left(\frac{q}{\epsilon} \right) (N_D - N_A + p - n) \quad (1)$$

where the donor and acceptor concentrations, N_D and N_A , are given functions of position. The mobile carrier densities are related to ψ , and to n_i , the concentration of carriers in intrinsic material, by the Boltzmann relations which apply to non-degenerate materials:

$$\begin{aligned} p &= n_i \exp \beta (\phi_p - \psi) \\ n &= n_i \exp \beta (\psi - \phi_n) \end{aligned} \quad (2)$$

where $\beta = q/KT$ while ϕ_p , ϕ_n denote the quasi-Fermi level potentials for holes and electrons which coincide with the Fermi level potential ϕ for equilibrium conditions but differ by an amount equal to the externally applied bias voltage in the quasi-equilibrium case corresponding to a system in the presence of such bias but with insignificant current flow.

As no method for the analytic solution of equation (1) is available problems of this type have usually been treated in terms of a combination of two approximate solutions⁽¹⁾, appropriate to different regions within the system, based, respectively, upon assumptions of (i) space-charge neutrality, $p - n = N_A - N_D$, and (ii) complete depletion of mobile carriers, $p \doteq n \doteq 0$.

The essential feature of such approximate solutions consists of the sudden transition, at the edge of the depletion region, from mobile carrier concentrations providing complete neutralisation of the fixed impurities to zero concentration. Within the depletion layer the potential is thus governed entirely by the fixed impurities.

It has recently been demonstrated⁽²⁾ that, in principle, any semiconductor system under equilibrium or quasi-equilibrium conditions in which

* A complete list of symbols is given at the end of the paper.



the mobile carrier densities are given by eq. (2) can be represented by means of a resistance network in which non-linear elements are associated with each mesh point. Such a representation is 'exact' in the sense that the difference equation which governs the potential distribution in the network becomes identical, for the limit of vanishing mesh interval with the Shockley-Poisson equation (1). In reference 2 preliminary results were reported, obtained on representations of two simple p-n junction geometries, namely the abrupt junction and the linearly graded one. A comparison between the analogue solution for the latter case and a numerical solution obtained by Morgan and Smits⁽³⁾, indicated good agreement between the two.

In the present paper, after a brief review of the analogue method, some of the practical considerations entering into the design and construction of this type of resistance network are discussed. These are followed by results obtained for a system geometry representing a diffused type p-n junction. Finally, the question of the feasibility of an extension of the method to current-carrying systems is considered.

2. Analogue treatment of equilibrium and quasi-equilibrium systems

As indicated above and discussed in detail in reference 2, the general relationship for a resistance network of constant mesh resistance R is given by (4,5,6,7,8)

$$\nabla^2 V^*(x^*) = - R I(x^*) \quad (3)$$

where $V^*(x^*)$ denotes the potential of the x^* th node and $I(x^*)$ equals the current entering this node. Equation (3) is transformed into a relationship corresponding to equation (1) by letting I consist of the sum of two components which are made to represent, respectively, the net mobile carrier concentration, p-n, and the net fixed charge density $N_D - N_A$.

The p-n term is a function of V^* and of two fixed potentials, ϕ_1 , ϕ_2 which simulate the quasi Fermi levels ϕ_p , ϕ_n . The fixed charge term will depend only upon the system geometry and will represent the impurity concentration at the point x in the physical system which corresponds to x^* in the analogue.

Thus,

$$I(x^*) = I_1(V^*(x^*), \phi_1, \phi_2) + I_2(x^*) \quad (4)$$

Resistance network solutions for problems of this type involving voltage dependent terms can be obtained by one of three methods: (i) network elements with the required voltage-current characteristic can be associated with each node so that the network potential will immediately

adjust itself to the required solution^(9,10), (ii) the current flow into each node may be manually adjusted as part of a procedure of successive approximations until the current value at each node bears the required relation to the potential at that node, (iii) the current adjustment may be carried out automatically, either simultaneously at all nodes, or iteratively, by means of standard analogue computing techniques^(11,12).

The work described in this paper is based upon the use of method (i), semiconductor diode groups providing the required non-linear circuit elements. The arrangement is illustrated schematically in fig. 1. Over the region in which the diode characteristic is adequately represented by its ideal form

$$i = i_s (\exp \beta^* V - 1) \quad (5)$$

β^* : empirical parameter $\approx q/KT$
 i_s : reverse saturation current

I_1 will be given by

$$I_1 = i_s \{ \exp[\beta^*(\phi_1 - V^*)] - \exp[\beta^*(V^* - \phi_2)] \} \quad (6)$$

as required by equation (2). The current flowing from the ϕ_1 line through the diode into the node at x^* will thus represent the hole concentration p , while that flowing from the node into the ϕ_2 line will represent n , the electron concentration.

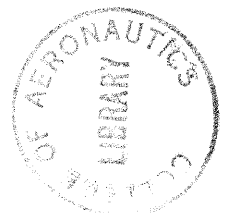
The current which constitutes the analogue to the fixed impurity density, properly scaled, is given by

$$I_2(x^*) = i_s \frac{N_D(x) - N_A(x)}{n_i} \quad (7)$$

while the scale factor relating the distance co-ordinate x in the physical system to x^* , the distance co-ordinate in the analogue (chosen so that $\Delta x^* = 1$ for neighbouring nodes) becomes⁽²⁾

$$\frac{x^*}{x} = \alpha = \left(\frac{1}{R} \frac{q}{\epsilon} \frac{\beta}{\beta^*} \frac{n_i}{i_s} \right)^{\frac{1}{2}} \quad (8)$$

For an analogue system using germanium diodes ($i_s \approx 10^{-6} \text{A}$) which represents a germanium system ($\epsilon = 16\epsilon_0$, $n_i = 2.5 \times 10^{-13} \text{cm}^{-3}$), α is of the order of 10^5cm^{-1} for $R \approx 300 \text{ohm}$.



It is worth noting that an alternative method of simulating equation (1) with the aid of diode groups is feasible. The essential feature of this alternative consists of the use of diode groups in conjunction with an operational amplifier in accordance with standard analogue computing techniques (13), (14). Compared with the resistance network, the analogue computer would seem to suffer from the following disadvantages in this particular application:

- (i) Since the distance co-ordinate must be transformed to become the time axis, the analogue computer technique is restricted to the treatment of problems of one or at most two dimensions, the latter at the cost of greatly increased complexity.
- (ii) The system geometry, i.e. the donor and acceptor atom concentration profiles, would have to be set up in terms of a time-programmed function.
- (iii) The facility for static measurements provided by the simultaneous and continuous accessibility of the potential distribution at all mesh points of a resistance network would be lost.

3. Practical considerations

The use of semiconductor diodes as non-linear elements in the manner outlined above introduces a number of special requirements:

- (1) Since it is an essential feature of the method that the actual diode characteristic approximates closely to the ideal one (eq. (5)), the range of impurity and carrier concentrations which can be represented is limited by deviations from the ideal characteristic which are found to occur at high currents. This is illustrated, for the diodes used in the present analogue, in fig. 2, which represents a typical current-voltage plot. Deviations can be seen to occur at currents exceeding 10mA, i.e. $\approx 10^4 i_s$.

As the region of primary interest in the type of problem under discussion is the high field region near the centre of a p-n junction, where impurity and carrier concentrations are low, this shortcoming of actual diodes does not represent a serious obstacle, although more 'ideal' diodes will extend the range of applicability of the network method.

- (2) As impurity concentration levels of practical interest may vary from $1 n_i$ to, say, $10^9 n_i$, different choices of i_s will be appropriate to different situations in view of the deviations from the ideal diode characteristics just mentioned.
- (3) Since i_s , the diode reverse saturation current, and β^* , the parameter characterizing the forward characteristic, enter into the analogue

equations and determine the scale factors for currents and distance, it is necessary, in principle, to use identical diodes. This requirement is met in practice by the use of diode groups, assembled from selected units, so that the characteristics of each group (rather than of each diode) are identical.

- (4) On account of the strong temperature dependence of i_s it is essential to place the diode groups within an environment which provides close control of the ambient temperature.

These considerations have led to the adoption of a design for the analogue system which combines the essential feature of diode temperature control with the maximum versatility regarding the resistance network layout. The diode groups are mounted upon plug-in printed-circuit type cards in such a manner that the entire array, which can accommodate a maximum of 312 diode groups, fits into a constant temperature enclosure. Each diode group is brought out to separate terminals on the front panel and the resistance network is set up in patch board fashion on these terminals. This type of construction permits the wiring-up of different system geometries of one, two or three dimensions without any disturbance of the diode groups. At the same time access to individual diode groups is maintained for test purposes, and the formation of compound groups, as required for use with graded mesh networks, is made easy.

4. Results: Diffused junction geometry

Whereas the results reported previously⁽²⁾ were obtained from analogue representations of two idealised p-n junction geometries, namely of the abrupt and the linearly graded junction, the measurements presented now relate to a junction structure formed by the superposition, upon a uniform acceptor atom concentration, of a donor atom concentration which falls off with distance according to a complementary error function law. This type of impurity distribution is of practical interest since it arises as a result of the diffusion method of p-n junction fabrication.

The complete system represents a combination of a highly doped uniform n-type region, extending from $x = 1$, to $x = 10$ for which $N_D/n_i = 1.1 \times 10^4$, a moderately doped region of low uniform acceptor density, $N_A/n_i = 40$, which extends from $x^* = 10$ to $x^* = 60$, and the non-uniform donor profile characterised by the expression $N_D(x^*) = 10^4 \text{cerf}(x^*/L^*)$ with $L^* = 11$. This combination of impurity profiles results in the formation of a highly asymmetrical p-n junction near $x^* = 33$. A graphical representation of the net impurity concentration is contained in figs. 6 and 7.

The potential profiles obtained from this resistance network representation are shown in fig. 3, for the case of zero bias, and for two reverse bias conditions over the region $x^* = 20$ to $x^* = 60$. (In the

region $1 \leq x^* \leq 20$ space charge neutrality prevails).

Numerical differentiation of the potential data yields the distribution of the electric field intensity throughout the system since

$$E = - \frac{dV^*}{dx^*} \cdot \frac{x^*}{x} .$$

In fig. 4 graphs of E are shown for the zero bias case and for two values of reverse bias. The dotted regions of the curves, in the interval $x^* = 10$ to $x^* = 26$ are based upon potential data from which fluctuations due to non-uniformities of the high current portions of the diode characteristics have been eliminated, the remaining parts were obtained by direct differentiation of the experimental values. The figure indicates clearly the increase, with increasing reverse bias, of the maximum field and of the width of the high field region.

Figures 5 and 6 show, in addition to the impurity profile already referred to, the concentration of mobile carriers for the zero bias case, and for a reverse bias of 4.0 volts. The widening of the space charge layer with reverse bias is clearly shown as is the fact that the space charge layer extends predominantly into the region of low impurity concentration. If the depletion region is defined, arbitrarily, as the region within which the mobile carrier density amounts to less than one fifth of the fixed charge concentration, its width is seen to equal approximately 2.5 x^* units at zero bias, 25 x^* units for 4 volt reverse bias.

5. Systems in presence of current flow

One limitation to the applicability of the analogue technique just described arises from the restriction to quasi-equilibrium conditions. This precludes the investigation of situations in which current flow significantly alters the mobile carrier concentration pattern, such as exist, for example, in strongly forward biased p-n junctions, in p-intrinsic-n junctions, or in transistors operating at high levels of injected carrier density. In this section the problems involved in an extension of the basic analogue method to the treatment of such non-equilibrium situations are considered and means for their solution proposed.

The current flowing within a semiconductor represents the sum of electron and hole currents, each of which is comprised of a drift and a diffusion component. For a one-dimensional system this leads to equations (1)

$$\begin{aligned} I_p &= q\mu_p p E - q D_p \frac{dp}{dx} = - q\mu_p p \frac{d\phi}{dx} \\ I_n &= q\mu_n n E + q D_n \frac{dn}{dx} = - q\mu_n n \frac{d\phi}{dx} \end{aligned} \quad (9)$$

which indicate that the total hole current and the total electron current are each proportional to the product of the local carrier concentration and the gradient of the appropriate quasi-Fermi level.

The complication introduced into the analogue treatment of the system by the presence of current flow can thus be seen to consist of the necessity to accommodate quasi-Fermi levels which vary with position, in place of the constant quasi-Fermi levels which characterized the equilibrium and quasi-equilibrium cases. If ϕ_p and ϕ_n were known functions of x , this change would introduce little difficulty; in place of the two common reference potentials to which all diode groups are connected in the equilibrium cases, distinct potentials $\phi_p(x^*)$, $\phi_n(x^*)$ would be applied to each diode group as indicated in Figure 7. As before, the resistance network potential $V(x^*)$ would represent the solution of the Poisson equation appropriate to this situation.

In practice, of course, ϕ_p and ϕ_n are not known as explicit functions of x . The spatial variation of the quasi-Fermi levels is governed by the requirement that the following conditions must be fulfilled:

- (i) constancy of total current $I_p + I_n$
- (ii) divergence of hole and electron current density vectors determined by prescribed local electron-hole recombination rates.

As shown in Reference 1, the complete analysis of the problem, i.e. the determination of $\phi_p(x)$, $\phi_n(x)$ and $\psi(x)$, requires the solution of the system of equations

$$\frac{d^2\psi}{dx^2} = \frac{q}{\epsilon}(p - n + N_D - N_A) \quad (10)$$

$$I_p = I - I_n = -q\mu_p p \frac{d\phi_p}{dx} \quad (11)$$

$$\frac{dI_p}{dx} = -qU \quad (12)$$

U , the net rate of electron-hole recombination, will itself depend upon p , n , and the density and energy levels of the centres involved in the recombination process. (15)

Differentiation of (11) yields

$$\frac{dI_p}{dx} = -q\mu_p \left(\frac{dp}{dx} \frac{d\phi_p}{dx} + \frac{d^2\phi_p}{dx^2} p \right)$$

which, upon substitution in (12) and use of the Boltzmann relations for carrier densities, $p = n_i \exp[\beta(\phi_p - \psi)]$, $n = n_i \exp[\beta(\psi - \phi_n)]$ leads to

$$\frac{d^2\phi_p}{dx^2} = \frac{U}{\mu_p p} - \beta \frac{d\phi_p}{dx} \left(\frac{d\phi_n}{dx} - \frac{d\psi}{dx} \right) \quad (13)$$

and

$$\frac{d^2\phi_n}{dx^2} = -\frac{U}{\mu_n n} - \beta \frac{d\phi_n}{dx} \left(\frac{d\psi}{dx} - \frac{d\phi_p}{dx} \right) \quad (14)$$

As stated above, if functions $\phi_p(x)$, $\phi_n(x)$ and $\psi(x)$ obeying equations (10) (13), (14) can be found for given impurity concentrations $N_D(x)$, $N_A(x)$ and for a prescribed recombination function $U(x)$, then the problem of the current carrying semiconductor system is solved.

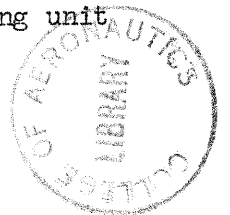
Now each of the three basic variables is governed by a differential equation of the form

$$\nabla^2\phi = f(\psi, \phi_p, \phi_n, U, N_D - N_A).$$

Since a resistance network provides analogue solutions to the difference approximation of this type of differential equation, an extension of the method used for the simulation of the quasi-equilibrium case suggests itself. In place of a single resistance network, three separate networks are set up, associated respectively with ψ , with ϕ_p , and with ϕ_n . Interconnections between these networks are provided in such a manner as to ensure that the current entering any node represents the corresponding term of the appropriate equation.

Figure 8 indicates schematically how this requirement can be met. Each ψ network is connected to diode groups which are returned to the quasi-Fermi reference voltages ϕ_p , ϕ_n in the manner described previously. In consequence, the potential distribution set up in the ψ network will as before, represent the solution to the Shockley-Poisson equation (eq. (1)). However, since ϕ_p and ϕ_n are themselves now derived from resistance networks, it is necessary to interpose buffer stages, B, between the nodes of these networks and the diode groups to prevent the current flowing through these from affecting the ϕ_p and ϕ_n potential distributions.

The required derivatives $d\psi/dx$, $d\phi_p/dx$, and $d\phi_n/dx$ may be computed for a particular set of node points (x^*_p) from the values of ψ , ϕ_p , and ϕ_n at neighbouring node points ($x^*_\pm 1, \pm 2$, etc.) in terms of finite difference approximations with an accuracy depending upon the highest order difference which is included in the computation. In the diagram, the three computing units 'D' perform these differentiations. An additional computing unit



('E') obtains the values of $U/\mu_p p$ and $U/\mu_n n$ from the values of ψ , ϕ_p , ϕ_n , and the constants governing the carrier generation - recombination process. In this manner all the information required for the evaluation of the terms on the right hand side of equations (13) and (14) is assembled, so that the two computing units shown as 'C' can evaluate $d^2\phi_p/dx^2$, $d^2\phi_n/dx^2$ and provide currents proportional to these terms to the x^k nodes of the ϕ_p and ϕ_n networks.

The somewhat excessive equipment requirements involved in such a threefold resistance network system can be scaled down very considerably if a system utilising a successive approximation method is adopted. This can be based upon the use of suitable storage devices, associated with each node of the ϕ_p and ϕ_n networks, by means of which the result of each successive computing step is impressed upon the potential distribution in the two networks.

6. Conclusions

The feasibility and usefulness of the resistance network analogue method for the evaluation of the characteristics of semiconductor systems in equilibrium or quasi-equilibrium has been demonstrated by the application of the method to the case of a diffused asymmetrical p-n junction. Data on potential profiles, electric field distribution and mobile carrier concentrations have been presented. The limitations of the method have been shown to lie in the restriction to situations involving constancy of quasi-Fermi levels thus implying absence of significant current flow.

It has been established that this limitation can, in principle, be overcome by a system comprising three resistance networks interconnected by analogue computing units. Such a combined system will provide a means for the analysis of steady state situations in current carrying semiconductor systems of arbitrary geometry and impurity profiles.

References

1. Shockley, W. The theory of p-n junctions in semiconductors and p-n junction transistors. Bell System Tech. J., Vol. 28, 1949, p. 435.
2. Loeb, H.W. An analogue method for the determination of potential distributions in semiconductor systems. J. Electronics Control, Vol. 14, 1963, p. 581.
3. Morgan, S.P., and Smits, F.M. Potential distribution and capacitance of a graded p-n junction. Bell System Tech. J., Vol. 39, 1960, p. 1573.

4. Liebmann, G. Solution of partial differential equations with a resistance network analogue. Brit. J. Appl. Phys., Vol. 1, 1950, p. 92.
5. de Packh, D.C. A resistor network for the approximate solution of the Laplace equation. Rev. Sci. Instr., Vol. 18, 1947, p. 798.
6. Gair, F.C. Unifying design principle for the resistance network analogue. Brit. J. Appl. Phys., Vol. 10, 1959, p. 166.
7. Redshaw, S.C. An electrical potential analyzer. Proc. Inst. Mech. Eng., Vol. 159, 1948, p. 55.
8. Garner, K.C. The potentiometer net; the basis of a new form of computer. Control, Vol. 6, 1963, p. 97.
9. Archard, G.D. Trajectory plotting in electron guns. Proc. Phys. Soc., Vol. 74, 1959, p. 177.
10. Redshaw, S.C., and
 Rushton, K.R. Various analogues incorporating negative resistances for the solution of problems in elasticity. Brit. J. Appl. Phys., Vol. 12, 1961, p. 390.
11. Karplus, W.J. The use of electronic analogue computers with resistance network analogues. Brit. J. Appl. Phys., Vol. 6, 1955, p. 356.
12. de Beer, A.J.F.,
 Groendijk, H., and
 Verster, J.V. The plotting of electron trajectories with the aid of a resistance network and an analogue computer. Philips Tech. Rev., Vol. 23, 1962, p. 352.
13. Holbrook, G.W. Hyperbolic analogs using varistors. Proc. IRE, Vol. 46, 1958, p. 1762.
14. Hellstrom, M.J. Hyperbolic analogs
 Proc. IRE, Vol. 46, 1958, p. 502.
15. Shockley, W., and
 Read, W.T. Statistics of the recombinations of holes and electrons. Phys. Rev., Vol. 87, 1952, p. 835.

Appendix

List of symbols

p	hole concentration
n	electron concentration
N_D	donor atom concentration
N_A	acceptor atom concentration
q	absolute value of electronic charge
ϵ	permittivity ($= k\epsilon_0$)
n_i	hole/electron concentration in intrinsic material
R	resistance network mesh resistance
k	Boltzmann's constant
T	absolute temperature
$\beta = q/KT$	
ψ	electrostatic potential in physical system
ϕ	Fermi level potential for system in equilibrium
ϕ_p, ϕ_n	quasi Fermi level potentials for system in quasi-equilibrium
x	distance co-ordinate in physical system
x^*	distance co-ordinate in analogue system
$\alpha = x^*/x$	
β^*	empirical diode forward characteristic parameter ($\beta^* \approx \beta = q/KT$)
i_s	diode reverse saturation current
V^*	potential in analogue system, representing ψ
ϕ_1, ϕ_2	reference potentials in analogue system, representing ϕ_p, ϕ_n



μ_p, μ_n mobility of holes, electrons
 D_p, D_n diffusion constant for holes, electrons
U net electron-hole recombination rate.

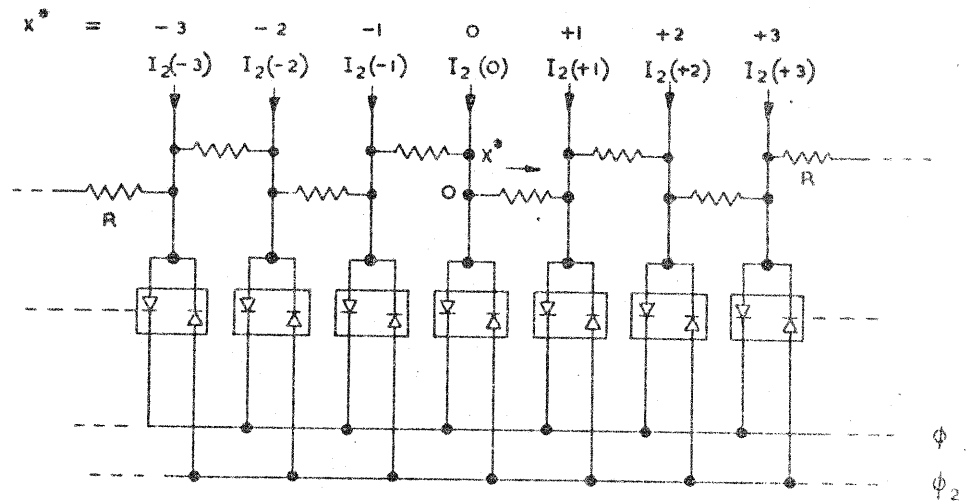


FIG. 1 RESISTANCE NETWORK WITH DIODE GROUPS AS NON-LINEAR ELEMENTS

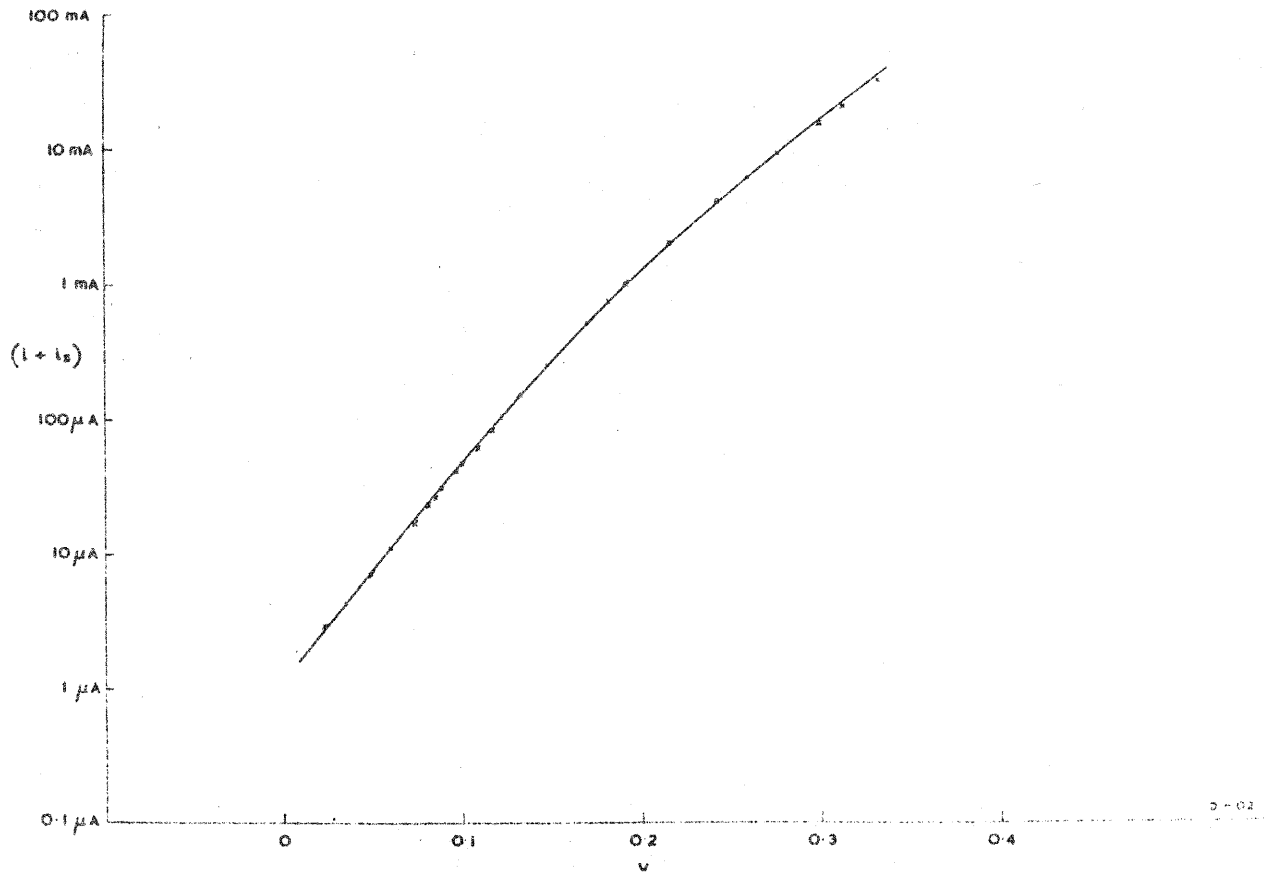


FIG. 2 PLOT OF $\ln(i + i_s)$ AGAINST V FOR DIODE GROUP USED TO REPRESENT MOBILE CARRIER CONCENTRATION DEPENDENCE UPON POTENTIAL

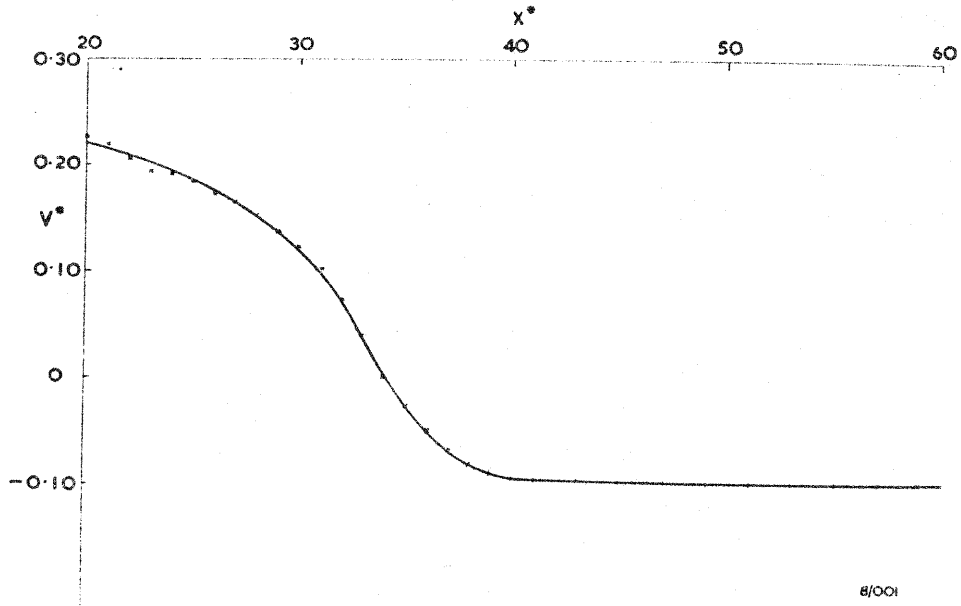


FIG. 3(a) POTENTIAL DISTRIBUTIONS OBTAINED FROM ANALOGUE: BIAS VOLTAGE 0V.

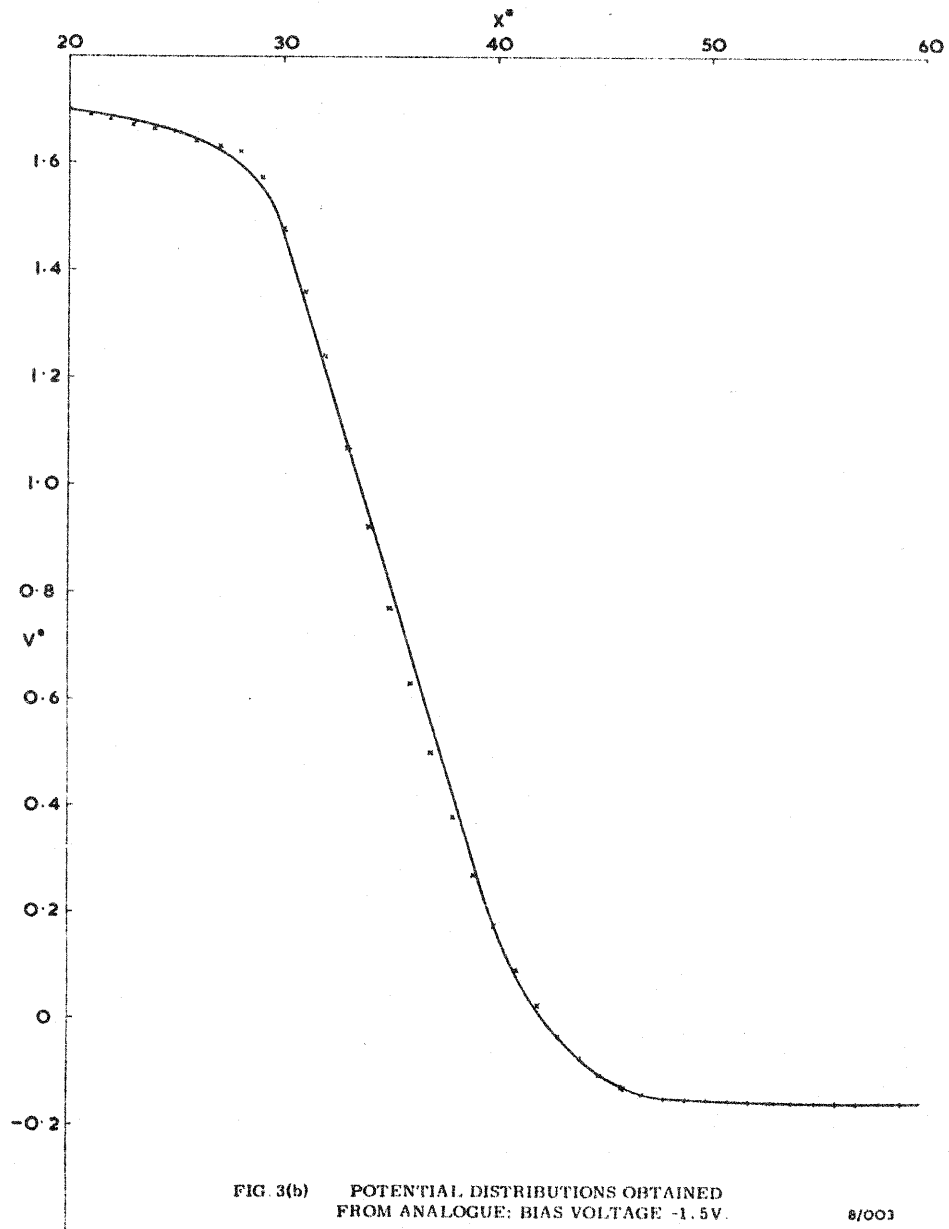
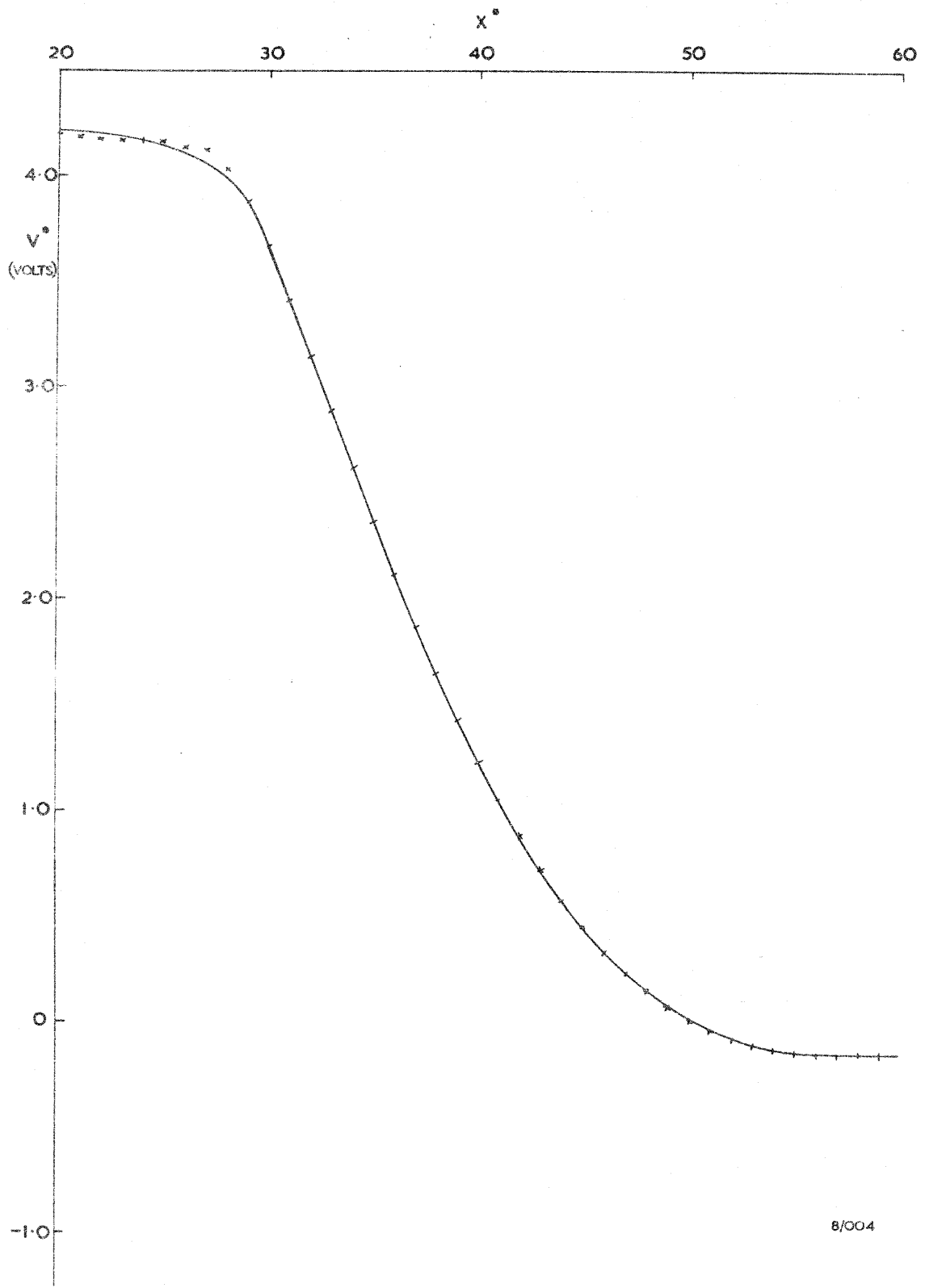


FIG. 3(b) POTENTIAL DISTRIBUTIONS OBTAINED FROM ANALOGUE: BIAS VOLTAGE -1.5V.



8/004

FIG. 3(c) POTENTIAL DISTRIBUTIONS OBTAINED FROM ANALOGUE: BIAS VOLTAGE -4V.

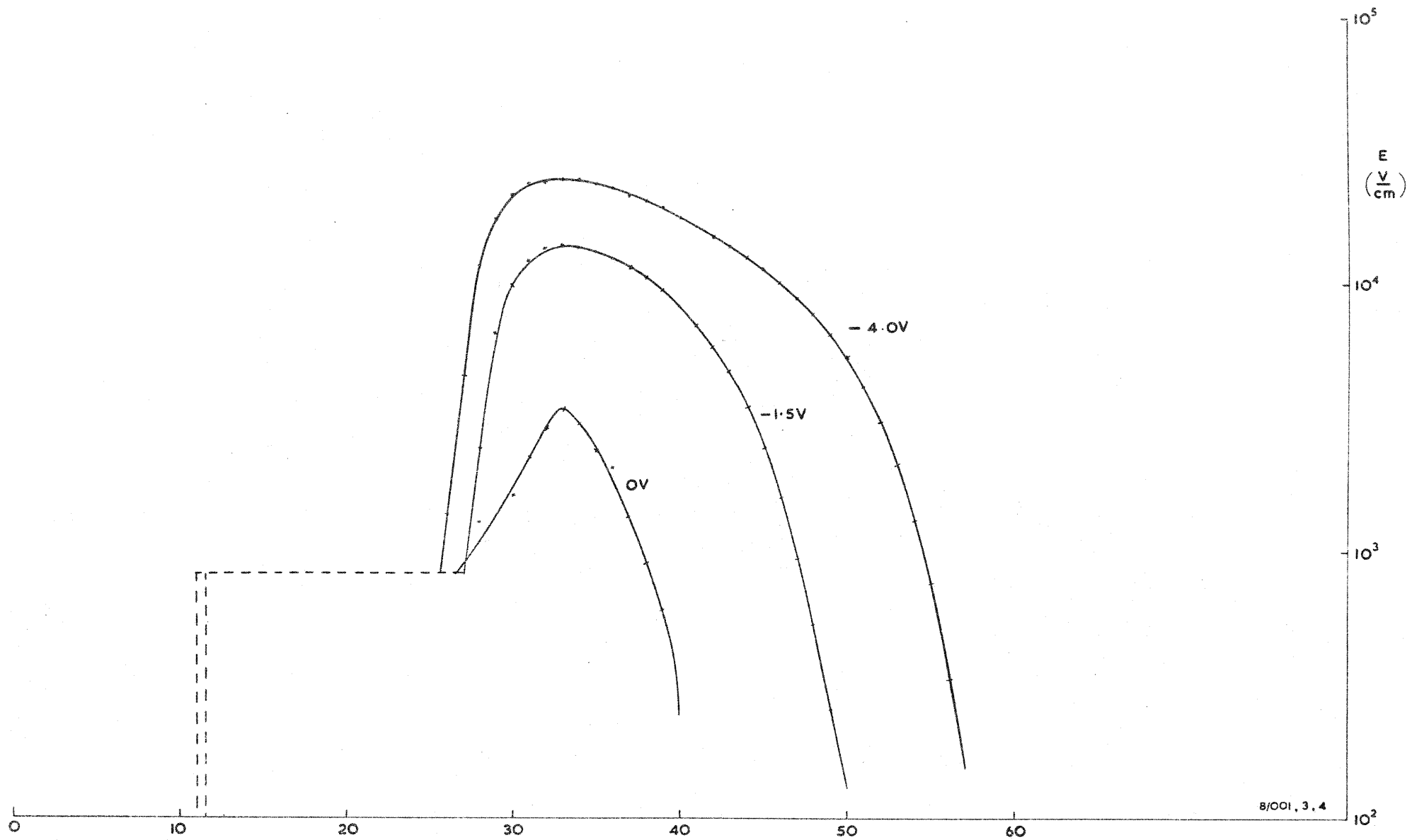


FIG. 4 ELECTRIC FIELD INTENSITY DISTRIBUTIONS FOR APPLIED BIAS VOLTAGES OF 0, -1.5 VOLTS, -4.0 VOLTS.

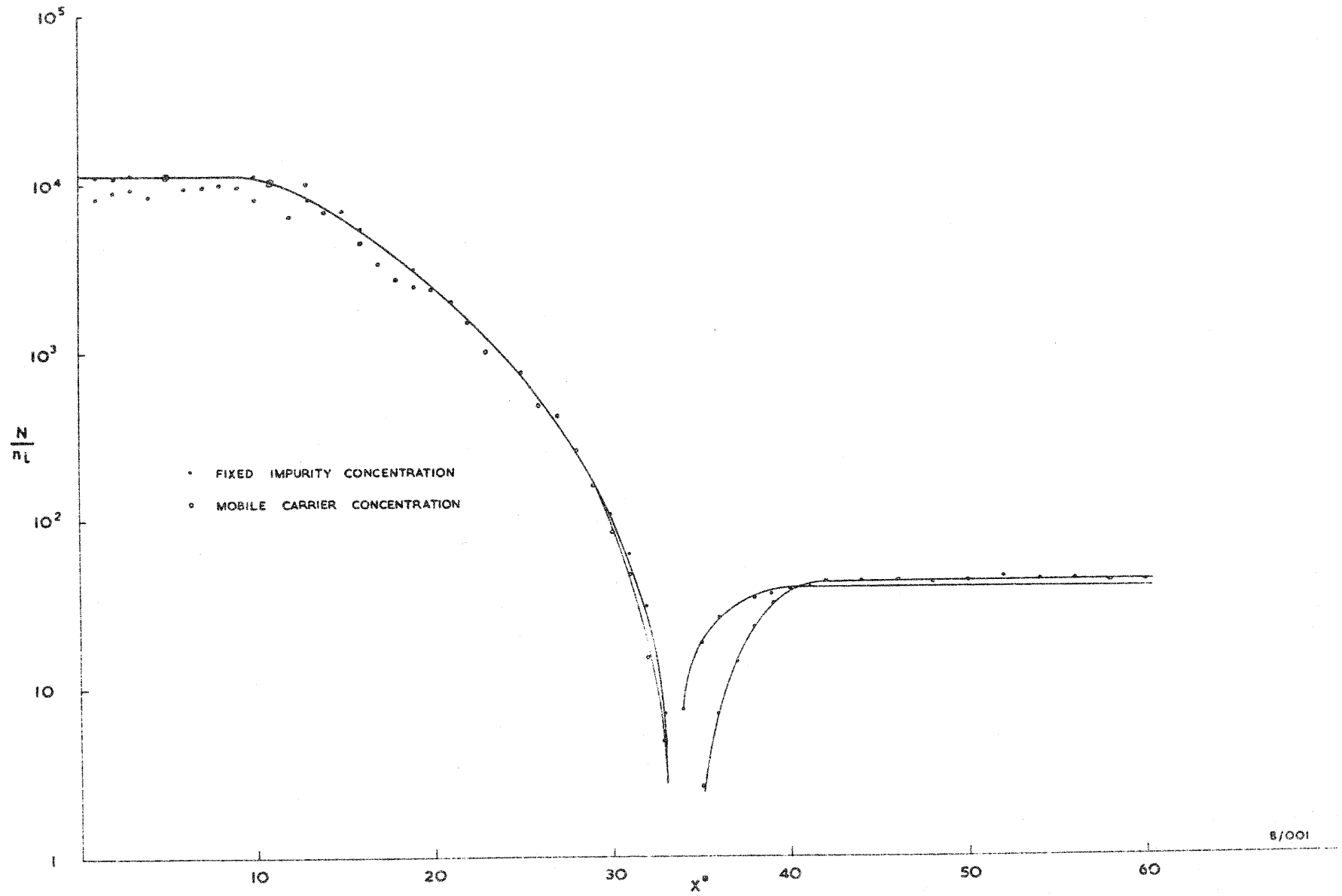
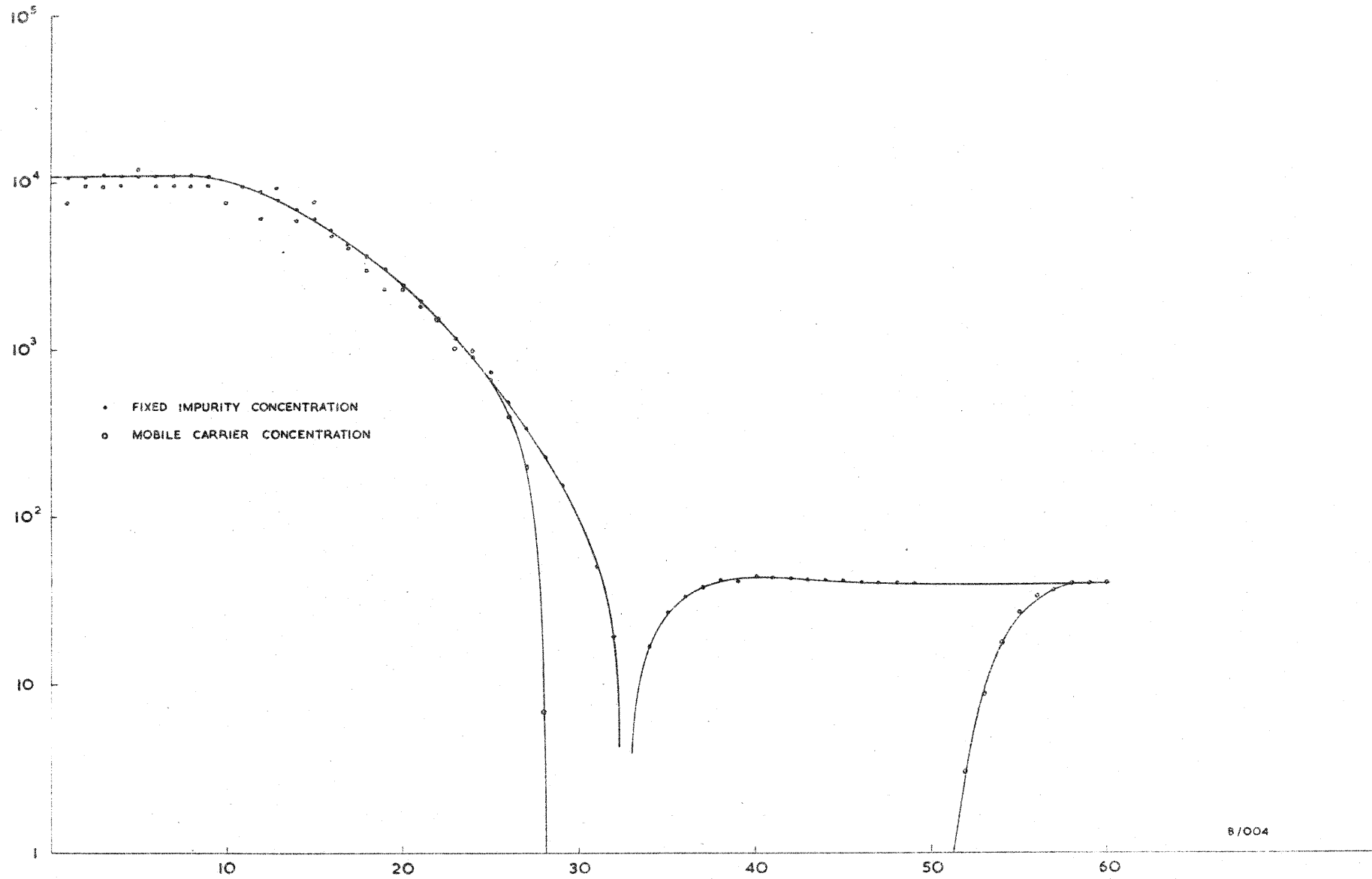


FIG. 5 IMPURITY PROFILE AND MOBILE CARRIER CONCENTRATION:
0 VOLT BIAS.



B/004

FIG. 6 IMPURITY PROFILE AND MOBILE CARRIER CONCENTRATION:
 - 4.0 VOLT BIAS.

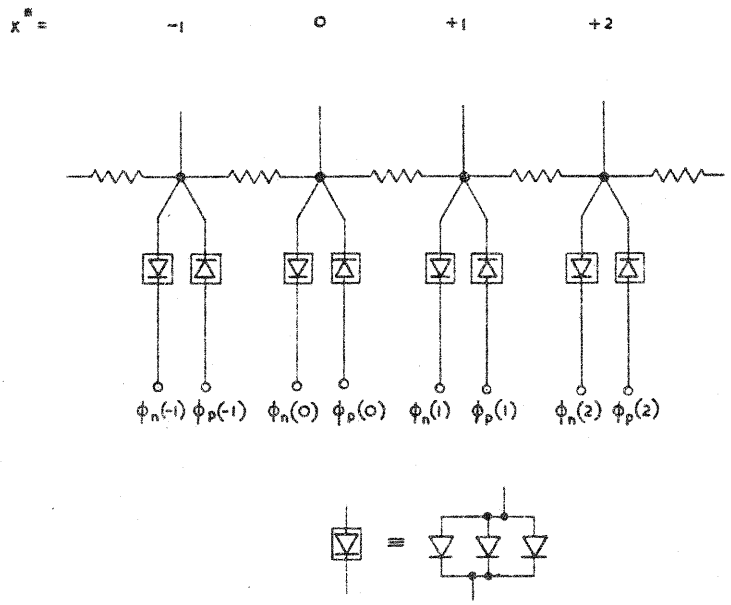


FIG. 7 ANALOGUE NETWORK FOR NON-EQUILIBRIUM SYSTEM

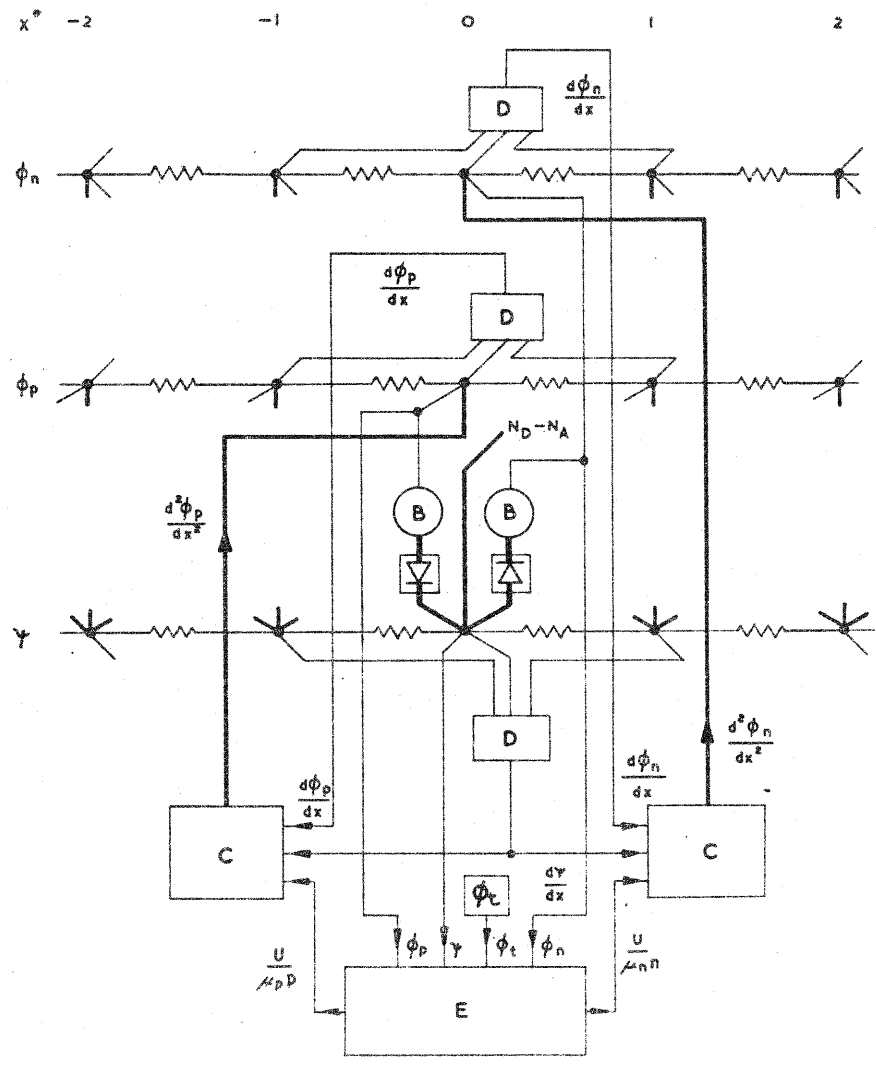


FIG. 8 INTERCONNECTION OF RESISTANCE NETWORKS TO PROVIDE CORRECT FUNCTIONAL RELATIONSHIPS FOR CURRENT-CARRYING SYSTEM.